Acta Geodyn. Geomater., Vol. 21, No. 1 (213), 27–36, 2024
DOI: 10.13168/AGG.2024.0003
journal homepage: https://www.irsm.cas.cz/acta

ORIGINAL PAPER

EXPLORE THE RELATIONSHIP BETWEEN SUNSPOT AREA AND SUNSPOT NUMBER WITH A NEW METHOD

Juan ZHAO

Department of Astronomy, Beijing Normal University, Beijing 100875, China

Corresponding author's e-mail: zj@bnu.edu.cn

ARTICLE INFO

Article history:
Received 28 November 2023
Accepted 18 January 2024
Available online 5 February 2024

Keywords:
Sunspot number
Sunspot area
Hemisphere
Global

ABSTRACT

There is a close correlation between sunspot number and sunspot area. Through the distribution of sunspot number and area size, we could note significantly disagreements for the two hemispheres. The paper concentrates on the relationship for the northern, the southern hemispheres and the global, and we propose a new method from segmentation regression for description the relationship between the sunspot number and sunspot area of different hemispheres and the global. By the sunspot number, we divide up the data into three parts, the low, the medium, and the high. The results indicate that the segmentation regression method could better describe the relation between sunspot area and number, in particular at the lower solar activity part and the higher part. We could obtain a better regression result for these parts, data more or less static, and data more discrete. Moreover, sunspot area and number behave very differently relationship for the north, the south and the global. In addition, the sunspot number being equal, the sunspot area of the south is usually greater than the north.

1. INTRODUCTION

Sunspots are dark regions on the solar surface that appear when strong magnetic fields suppress convection. It is often assumed that it is related to the solar dynamo models (Charbonneau, 2020). As the distinguishing external feature of solar activity, it seems to be somewhat synchronized with the changes of solar activity intensity, and is broadly used in space environment, the solar-terrestrial relation, and weather and climate (Solheim, et al., 2012; Nagovitsyn and Osipova, 2023).

Valid observational records of sunspot number follow the development of telescope, and the really long continuous record started by Wolf (1861), from 1849 to the present (Schröder, 1997; Casas et al., 2006; Hathaway, 2010). Sunspot number was used a united formula during counting, but the shape and size of sunspots are really irregular. As a matter of fact, sunspot area contains more information with respect to sunspot number (Ermolli et al., 2014; Zharkova and Shepherd, 2022). However, the observation of sunspot area, beginning in 1874, comes after the sunspot number.

Astronomers have been figuring out what sunspot had to do with magnetic fields. In the presence of high temperature in solar interior, the substance comes in plasmas. The fluid motion of the plasma impact on the distribution of magnetic field, which in turn impact on the fluid motion meanwhile (Babcock, 1961). The temperature decreases from edge to center progressively in sunspot region. As for the cooling of sunspot region, it is believed that the strong magnetic field generated by the dense magnetic field lines is related. However, the existence of strong magnetic field inhibits the convection of the fluid in the plasma state, resulting in low temperature. The fact that sunspots are magnetic fields accounts for their dark appearance. The magnetic field strength is related to sunspot area. That is to say, sunspot area has much more important meaning of what can be thought that reflects solar magnetic activity with better feature characterization.

It is valuable to explore the linkage between sunspot number and sunspot area, correlated well with each other, enable us to go further for the research of solar activity (Krivova et al., 2007; Clette et al., 2014). Not only now, but, on some level data reconstruction of solar activity it always is the key element of solar physics research, especially the historic data. We could reconstruct for other index with shorter records, such as sunspot area, as well using sunspot number, even provide valuable information for forecasting that is really an important direction of solar activity research (Zhao and Han, 2012).

Previous oft-quoted relationship between sunspot number and area is based on the global data. There were very few researches to even touch it based on hemispheres. The paper explores the relation

Cite this article as: Zhao J: Explore the relationship between sunspot area and sunspot number with a new method. Acta Geodyn. Geomater., 21, No. 1 (213), 27–36, 2024. DOI: 10.13168/AGG.2024.0003

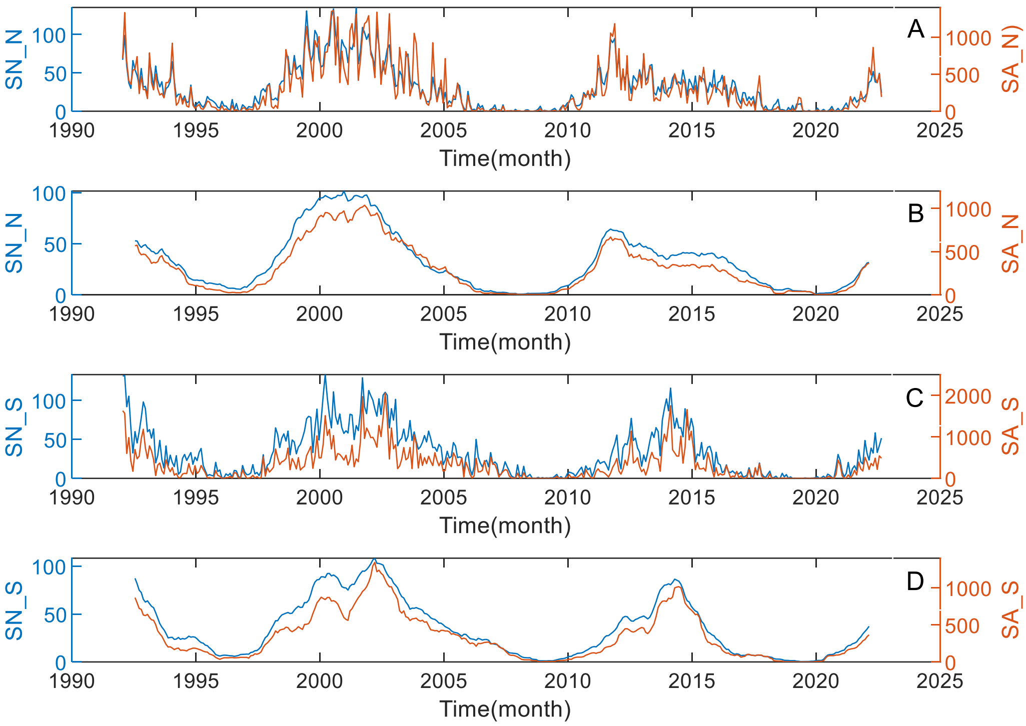

Fig. 1 The time series of international sunspot number and sunspot area from 1992.1 to 2022.8 for the two hemispheres. The sunspot numbers are plotted here as the monthly averages (A, C: blue), and 13-month smoothed monthly average (B, D: blue). The sunspot areas are plotted here as the monthly averages (A, C: orange), and 13-month smoothed monthly average (B, D: orange). The unit of SA is one millionth of the solar total area. Panel A, B focus on the northern hemisphere, and panel C, D are for the southern hemisphere.

linkage between sunspot number and sunspot area at different intensity of solar activity relying on the segmentation method and studies the characteristics and change rules of the relationship. This paper is organized as follows: the first part gives the data sources and describes their temporal evolution. The second part is the comparison analysis through the difference, the ratio, and the distribution. The next part introduces the segmentation regression method and compares them to other research. The last part concludes, discusses, and anticipates further research.

2. CHANGE OF SUNSPOT NUMBER AND SUNSPOT AREA

The hemispheric Sunspot Numbers (SN) in 1-month interval are obtained from WDC-SILSO, Royal Observatory of Belgium from January 1992 to August 2022 (http://www.sidc.be/silso/). The primary hemispheric Sunspot Area (SA) data used in the present study is obtained from the website, (https://solarcyclescience.com/activeregions.html) for the period 1992.1–2022.8, summarized by Dr. L. Upton and Dr. D. Hathaway, contains the combined Greenwich Royal Observatory (RGO) and Solar Optical Observing Network (SOON) data.

We can see the data changes of monthly hemispheric SN against SA in Figure 1. In this figure, it is clear that they have a similar variation trend and a strong correlation. Monthly series have been less volatile than the daily series, but we can see that whether sunspot number or sunspot area, still keep on waving greatly, especially at peak positions. These fluctuations will harm for observing double-peaked structure and so on characteristics of variation. Therefore, we improve the two series for the two hemispheres by using 13-point moving average, semi-weight at the first and the last point. The smoothed series can well describe the variation characters of hemispheric sunspot number and area.

3. COMPARISON ANALYSIS

3.1. DIFFERENCE

We calculated the first order difference of sunspot number and area, respectively. It is shown in Figure 2 that the first order difference of SA varies along with it of SN for the two hemispheres, and the difference of sunspot area is steadily expanding along with the sunspot number increasing and approximately present linear growth relationship.

For the north, the regression equation was established as follows:

$$Dsa = (12.73 \pm 1.04)Dsn + (0.08131 \pm \pm 15.4287) \quad (1)$$

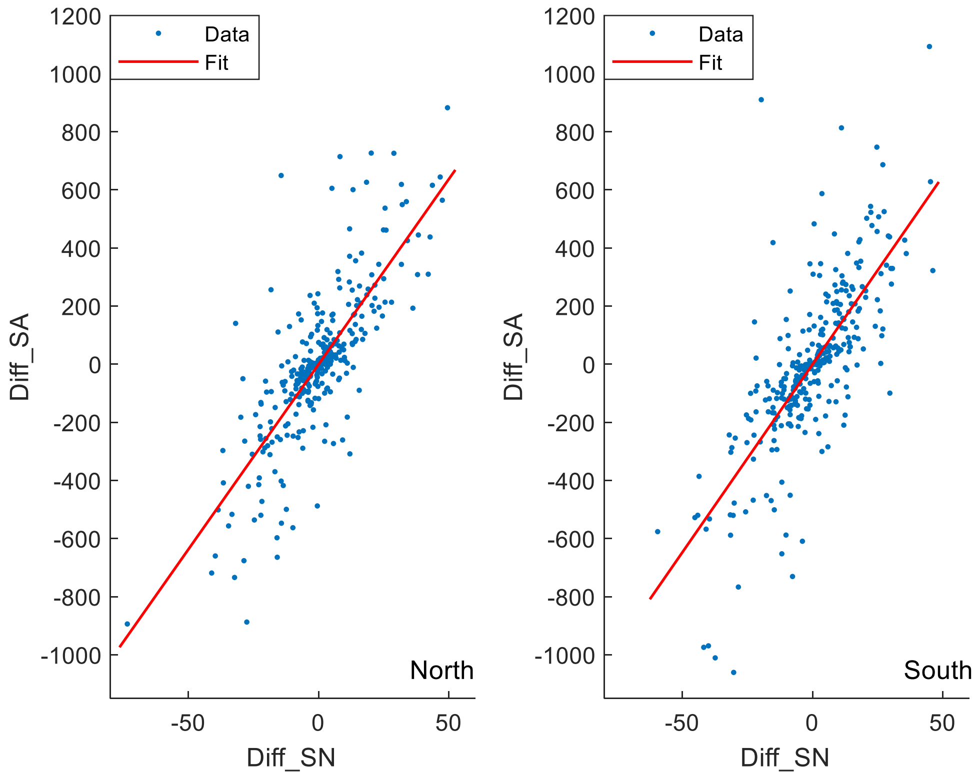

Fig. 2 Scatter plot of the first order difference of sunspot number and sunspot area for the northern hemisphere (Left panel) and the southern hemisphere (Right panel). The red line is the linear relationship between SN and SA.

where *Dsa* is the first-order difference of sunspot area, and *Dsn* is the first-order difference of sunspot number. Here, given coefficients with 95 % confidence bounds. The value of the Pearson correlation coefficient *r*, 0.785, is higher than the 99.9 % confidence level, and *F*-test value is 585.77.

For the south, the regression equation is

$$Dsa = (12.94 \pm 1.18)Dsn - -(0.3085 \pm 17.9585) \tag{2}$$

with *F*-test value is 460.2317. The correlation coefficient *r*, 0.747, is higher than 99.9 % confidence level.

We perform the regression test thoroughly with polynomial. If use a quadratic polynomial here, the quadratic coefficient is a tiny value, and if use a cubic polynomial, the quadratic and cubic coefficients are tiny values. And it's roughly the same R^2 and root-mean-square error (RMSE) of all three. Therefore, we can credibly describe the relation between the difference of sunspot number and it of sunspot area shows the linear regression for whichever hemisphere. That is, in any case, sunspot area varies with sunspot, but the rate of growth of both is the linear relationship.

3.2. RATIO

We calculated the ratio between SA and SN for the two hemispheres, respectively. These ratios register the fluctuations of sunspot area over the number for different hemisphere. Then, to better explore the trend, we gave the smoothed ratio after 13-point moving average, shown in Figure 3, it showed us plainly that the ratio for different hemisphere would not be the same.

The Maximum of the ratio for the north occurred at the descending part of the solar cycle, but it occurred at the valley for the south. For example, the ratio is larger near 2004, which been descending part of Solar Cycle 23, for the north. However, it is larger near 2007, which been the valley of Solar Cycle 23, for the south.

The ratio is not constant and varies with time. In addition, the ratio fluctuates greatly. The mean ratio of monthly data is 7.3316 and the median is 7.1967 for the northern hemisphere. But for the southern hemisphere, the mean is 7.7692 and the median is 7.7729. We can figure out that the ratio of the south is greater than it of the north, when we look at the mean and the median. This means that the sunspot number being equal, the sunspot area of the south is usually greater than the north.

Its dynamic curve appeared as period change feature that is interact results of period or un-period factors. Spectrum analysis reveals the primary period for the south is 122.667 month, and it's the same for the north. However, there is also an apparent period about 73.6 month for the north, as shown in Figure 4.

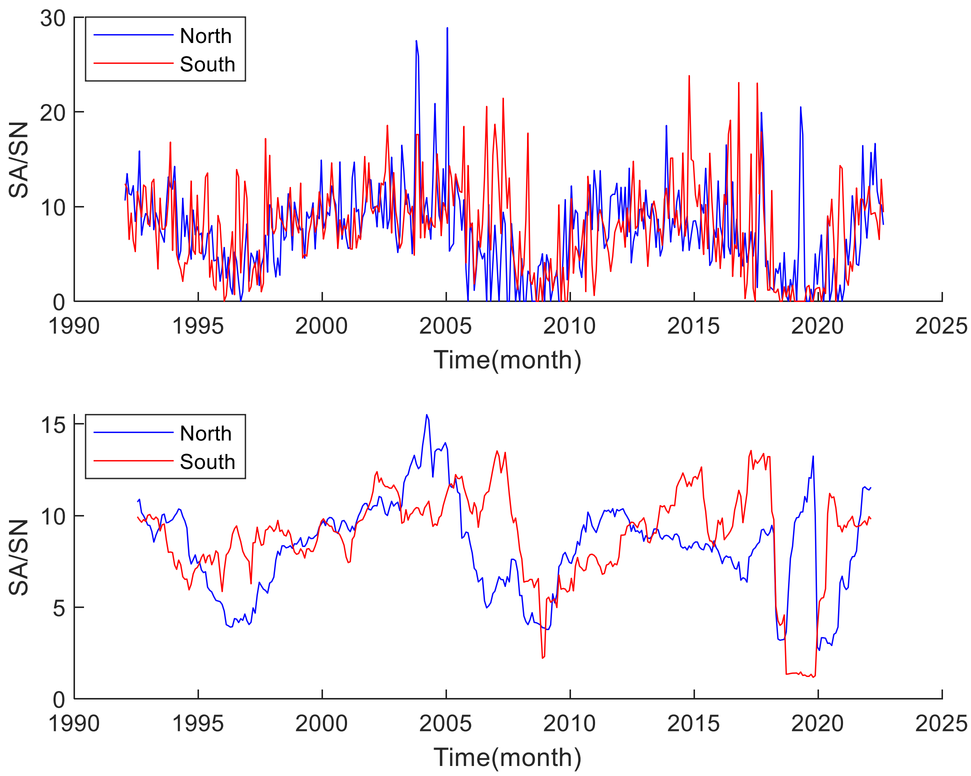

Fig. 3 The upper panel shows the original ratios between SA and SN for 1992.1-2022.8, while the lower panel shows the smoothed ratios.

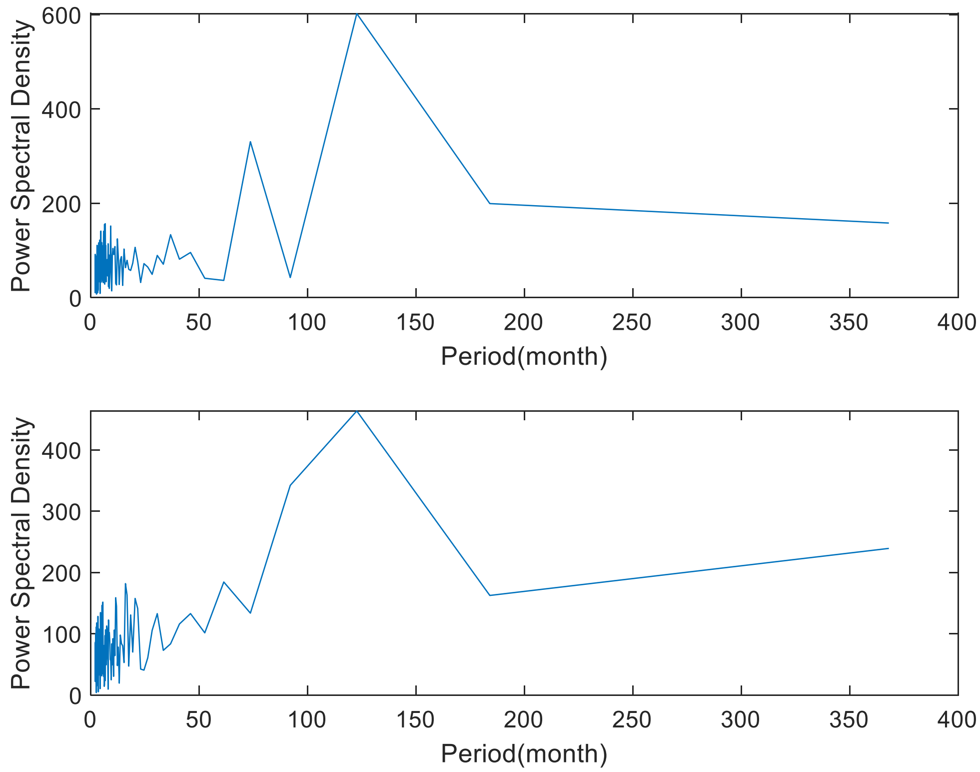

Fig. 4 The power spectrum of the ratio series for the northern (Top panel) and the southern hemispheres (Bottom panel).

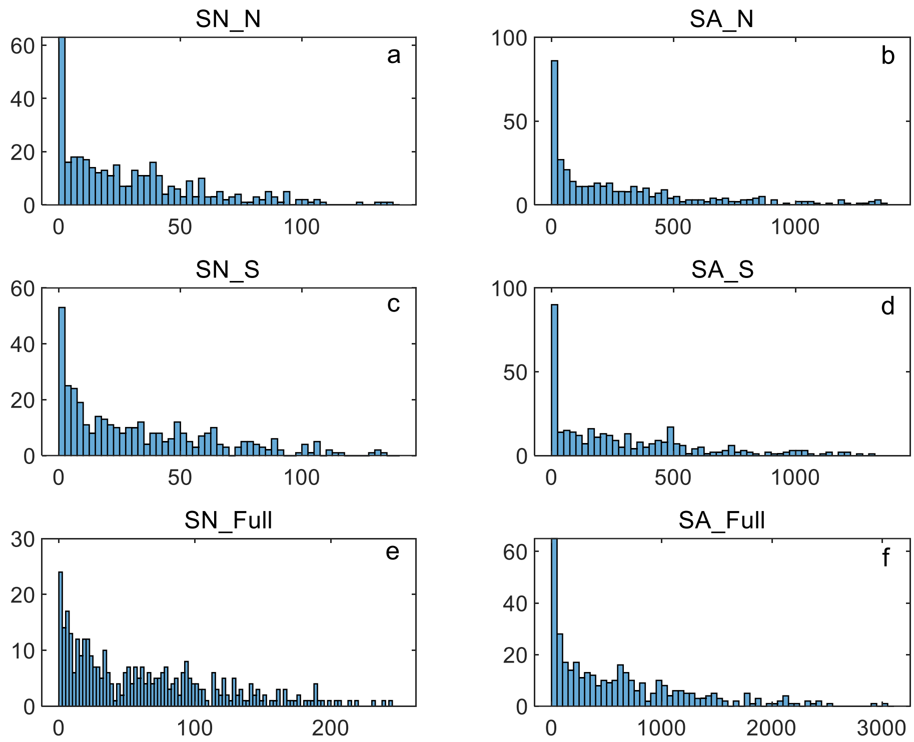

Fig. 5 Histogram of sunspot number (Left panel) and sunspot area (Right panel) for the northern hemisphere (a, b), the southern hemisphere (c, d), and the global (e, f).

3.3. DISTRIBUTION

There are 368 hemispheric samples for the interval 1992.1 to 2022.8. Here, we show the frequency distribution of sunspot number and area through histogram which is relatively straight forward for knowing about distribution (Fig. 5). So according to frequency value to determine the cut-off point, and we could really divide the sunspot number into three major parts. The month, that's sunspot number in fewer numbers, was in the low part. If it is in medium number, belong to the middle part, and if in large quantity, it is in the high part.

For the north (Figs. 5a, 6a), there are 63 samples ≤ 2.5, 53 samples > 60, and 252 samples between them. Here, 68.48 % samples are concentrated at the medium part from 2.5 to 60.

Likewise, we divide sunspot number for the south into 3 parts, ≤ 2.5, $2.5 < sn \leq 65$, >65, like the northern hemisphere (Figs. 5c, 6b). Different from the north, the SN of the southern hemisphere vary greatly and rarely appears around 65, therefore 65 is chosen as the cut-off point. There are 55 samples ≤ 2.5, 54 samples > 65, and 259 samples between them. Here, 70.38 % samples are concentrated at the middle part from 2.5 to 65.

According to the frequency distribution of the global sunspot number, we also divide them into 3 parts, ≤ 10, $10< sn \leq 107.5$, > 107.5, (Figs. 5e, 6c). There are 68 samples ≤ 10, 74 samples > 107.5, and 226 samples between them. Here, 61.4 % samples are concentrated at the middle part from 10 to 107.5.

Because this paper explores the process that the sunspot area changes with sunspot number, we divide the sunspot number into 3 parts only here, and don't talk about the cut-off point of sunspot area.

4. SEGMENTATION REGRESSION

Based on aforementioned 3 parts, the low part, the medium part, and the high part, of sunspot number, we proposed a way of "segmentation regression" to take regression analyses to discover the relationship between SN and SA for the two hemispheres and the global data respectively.

For different part, we regress in three ways, by linear regression, second-order polynomial, and third-order polynomial individually, as are compared in Figures 7 and 8. According to the comparison, we could easily make a distinction and choose the proper regression equation.

4.1. THE NORTHERN HEMISPHERE

As noted above, we choose 2.5 and 60 as cut-off points in the northern hemisphere regression process, and divide them into three parts: the SN less and equal to 2.5, between 2.5 and 60, and larger than 60.

Based on the regression results by three ways, and the linear relationship between the difference of SN and SA in section 3.1, we choose the quadratic polynomial as the segmentation regression function.

If the SN is less than or equal to 2.5, the equation derived from the quadratic polynomial regression analysis is

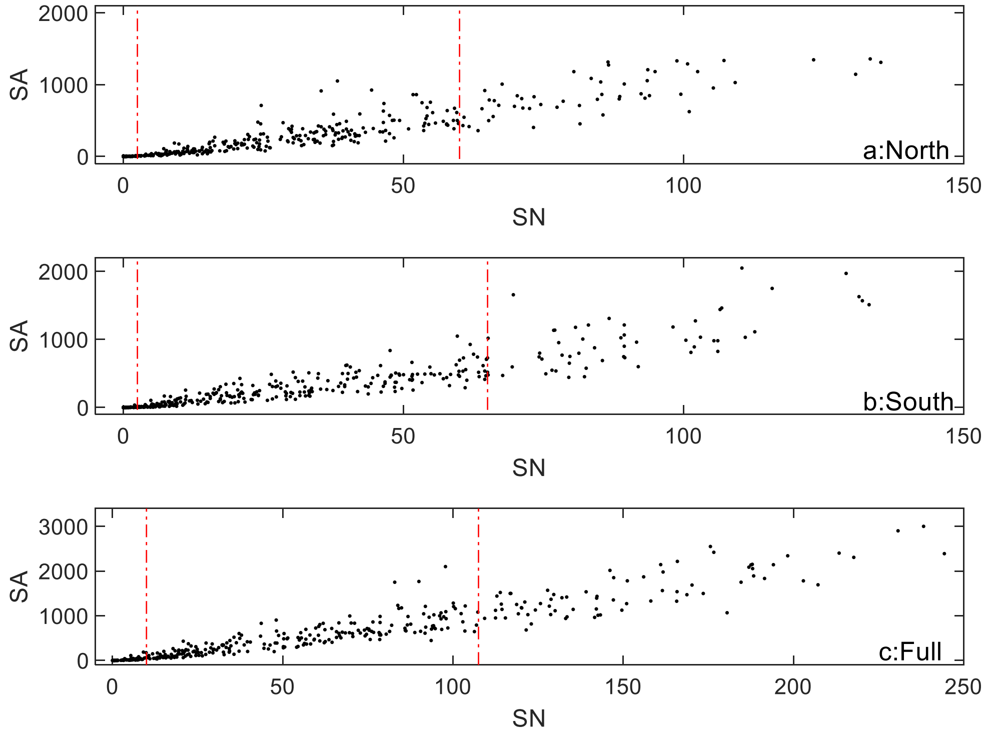

Fig. 6 Sunspot number *vs.* sunspot area. Red dash-dot lines are the dividing lines of three parts.

$$SA = (1.05 \pm 1.197)SN^2 - (0.2782 \pm \pm 2.6255)SN + (1.173 \pm 0.968) \quad (1)$$

The red line is the quadratic regression curve in Figure 7a. The coefficient of determination, R^2, is 0.3223 between the SA and SN. *F*-test value is 86.7932, at confidence level: P > 99.9 %.

If the SN is between 2.5 and 60, the regression equation is

$$SA = (-0.01151 \pm 0.05825)SN^2 + (10.97 \pm \pm 3.5)SN - (39.67 \pm 43.18) \quad (2)$$

The coefficient of determination, R^2, is 0.6771, and *F*-test value is 382.6905, at confidence level: P > 99.9 %.

When the SN is larger than 60, the regression equation is

$$SA = -(0.08365 \pm 0.1248)SN^2 + (26.29 \pm \pm 23.52)SN - (728 \pm 1072) \quad (3)$$

With *F*- test is 196.9968, at confidence level: P >99.9 %. The R^2 is 0.5191.

The red regression line is for the quadratic polynomial regression analysis (Figs. 7A, 7B, and 7C). We could note that the relationship between SA and SN shows different variation characteristics during three parts. And in the medium part, the quadratic coefficient is much lower than the first order coefficient, close to linear fashion. The segmentation regression could not only take the high value part into account, but also rise the accuracy of the low value part.

4.2. *THE SOUTHERN HEMISPHERE*

When the SN ranged from 0 to 2.5,

$$SA = (1.029 \pm 2.281)SN^2 + (1.273 \pm 5.258)SN - -(0.04157 \pm 2.081) \quad (4)$$

R^2 equals to 0.3001 between SA and SN. *F*-test value is 78.2515, at confidence level: P > 99.9 %.

When the SN is larger than 2.5, and less than and equal to 65,

$$SA = -(0.01268 \pm 0.0401)SN^2 + (10.22 \pm \pm 2.64)SN - (17 \pm 33.77) \quad (5)$$

R^2 is 0.7544. *F*-test value is 560.5782, at confidence level: P > 99.9 %.

When the SN is larger than 65,

$$SA = (0.1687 \pm 0.2321)SN^2 - (18.39 \pm \pm 45.59)SN + (1221 \pm 2178) \quad (6)$$

R^2 is 0.4544. *F*-test value is 151.9941, at confidence level: P > 99.9 %.

The red curve is the quadratic polynomial regression analysis (Figs. 7D, 7E, and 7F). The regression result in the medium part of the south was similar to the north, close to linear fashion. However, the variation characteristics in the low part and the high part are completely out of the north.

4.3. *THE GLOBAL*

As aforementioned, we also applied the quadratic polynomial segmentation regression, ≤ 10, $10 < sn \leq 107.5$, > 107.5, for the global data (Fig. 8).

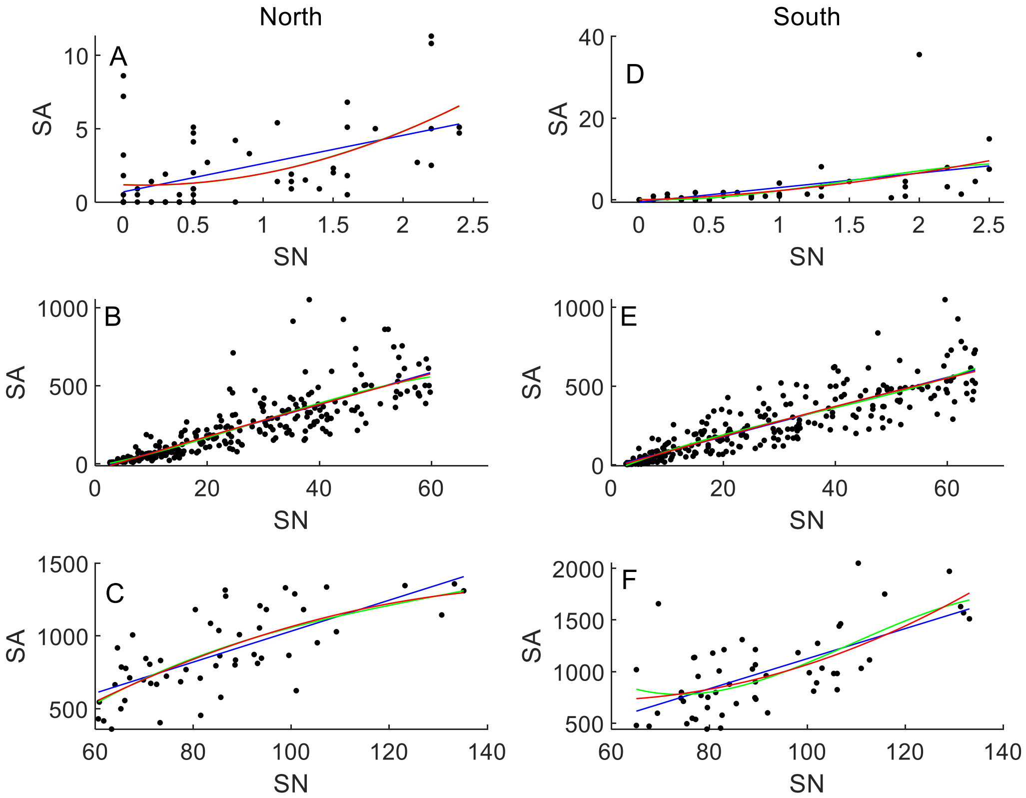

Fig. 7 The relationship between sunspot area and sunspot number for the northern hemisphere (left panel) and the southern hemisphere (right panel) for the period from 1992.1 to 2022.8. The blue solid line is the linear relationship between SN and SA. The red solid line is the quadratic regression curve. The green solid line is the cubic polynomial regression curve. (A.) The low part for the north; (B.) The medium part for the north; (C.) The high part for the north; (D.) The low part for the south; (E.) The medium part for the south; (F.) The high part for the south.

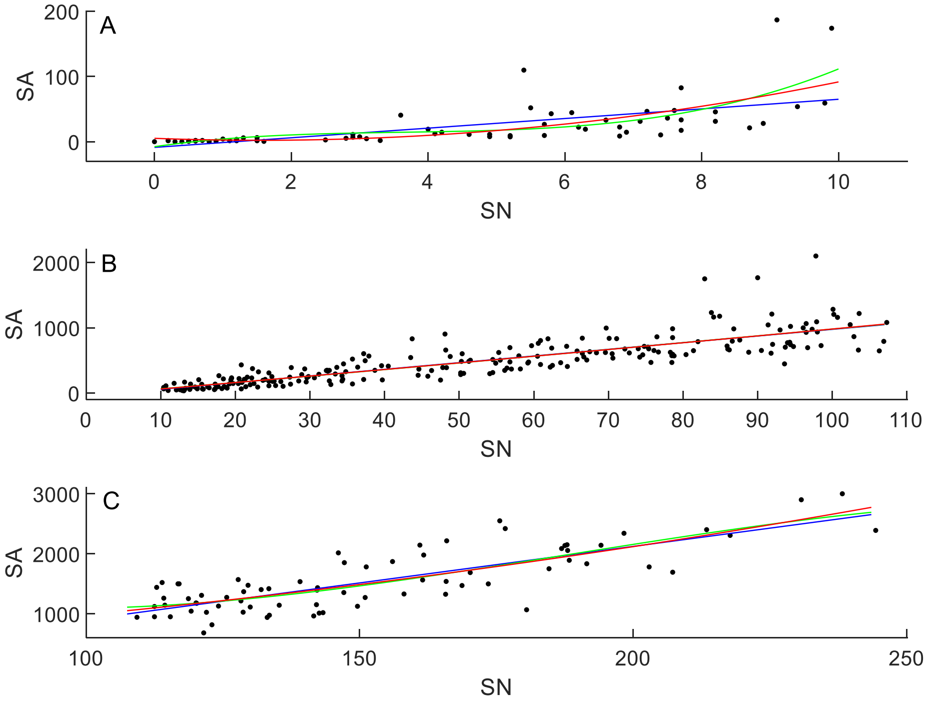

Fig. 8 The relationship between sunspot area and sunspot number for the global data for the period from 1992.1 to 2022.8. The blue solid line is the linear relationship between SN and SA. The red solid line is the quadratic regression curve. The green solid line is the cubic polynomial regression curve. A: the low part; B: the medium part; C: the high part.

Table 1 List of the previous studies of the relationship between sunspot number and sunspot area, and the corresponding formulae.

Study	Formula
Carrasco et al. (2016)	$SA=(2.5\pm1.0)SN^{(1.29\pm0.01)}$
Yury et al. (2021)	$SA=(4.51\pm0.30)SN^{(1.177\pm0.016)}$ (*a*)
Yury et al. (2021)	$SA=(5.18\pm0.56)SN^{(1.149\pm0.021)}$ (*b*)
Yury et al. (2021)	$SA=(0.0114\pm0.0017)SN^{2}+(9.08\pm0.29)SN$ (*c*)

For the low part,

$$SA = (1.253 \pm 0.856)SN^2 - (3.878 \pm 7.972)SN + +(5.14 \pm 14.35) \quad (7)$$

with R^2=0.4761, and F-test value is 165.8489, at confidence level: P > 99.9 %.

For the medium part,

$$SA = (0.004327 \pm 0.03595)SN^2 + (9.739 \pm \pm 4.069)SN - (36.18 \pm 94.32) \quad (8)$$

with R^2=0.7149, and F-test value is 457.6263, at confidence level: P > 99.9 %.

For the high part,

$$SA = (0.02567 \pm 0.05784)SN^2 + (3.652 \pm \pm 19.328)SN + (362.4 \pm 1555.6) \quad (9)$$

with R^2=0.6463, and F-test value is 333.4740, at confidence level: P > 99.9 %.

Regression in segmentations provides a better fit than the whole regression does, especially for fitting in the starts of abscissa, the part low in value.

4.4. COMPARE WITH OTHER STUDIES

The relation between sunspot area and sunspot number is once simply described as, $SA = 16.7SN$ (Kiepenheuer, 1953; Waldmeier, 1955). As scientists go on in research and the data length and accuracy have been further improved, the relation is not really a good linear fashion, as shown in Figure 8. Regarding formulae that describe the relationship, there isn't a universal formula because it is complex and varies along with time, and different researchers have applied various methods to model the relationship between SN and SA (Carrasco et al., 2016; Yury et al., 2021).

We can see these formulae in Table 1. We compare and analyze the segmentation regression results with the whole regression results from other researchers, shown in Figures 9, 10. Among these, Yury et al. (2021) gave 2 models based on Carrasco et al. (2016) and another polynomial model.

Figure 9 contrasts the segmentation regression results for the two hemispheres and the whole regression results. We can see that there are certain differences from different regression methods. Nor is this difference confined to the low and the high part as conventionally believed. The data-intensive medium part, too, has difference.

The greatest difference between segmentation and unsegmented regression exists in the high part. Therefore, requirements are higher in the part with more discrete data, and reliable equation could accurately reflect the variation characteristic sunspot area varying with sunspot number in the high part. Moreover, as aforementioned, the north and the south show totally different characteristics in the high part. Previous studies rarely make regression analysis for the hemispheres, and no one, until this time, had suggested the segmentation regression method. Therefore, we could only compare hemispheric results with other global results. The standard deviation of different regression methods prove that the segmentation method is the better irrespective of whether the north or the south. All these are listed in Table 2.

Table 2 The Standard Deviation (Std) from different methods for the two hemispheres and the global data.

Study	Std for the north	Std for the south	Std for the global
Zhao and Han (2012)	120.1476	138.4548	199.1995
Carrasco et al. (2016)	137.9434	159.7195	211.7696
Yury et al. (2021) a	123.5548	145.4656	209.7091
Yury et al. (2021) b	122.2389	144.3624	209.0203
Yury et al. (2021) c	122.1710	144.8811	207.7949

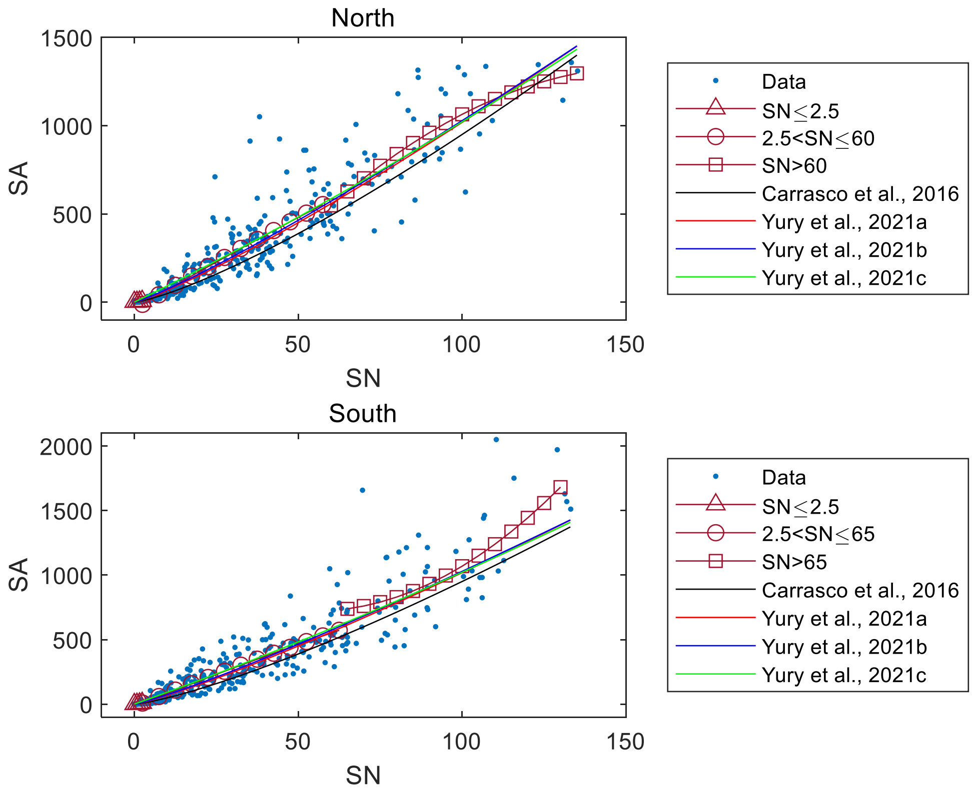

Fig. 9 Compare with other studies for the northern hemisphere (Top panel) and the southern hemisphere (Bottom panel).

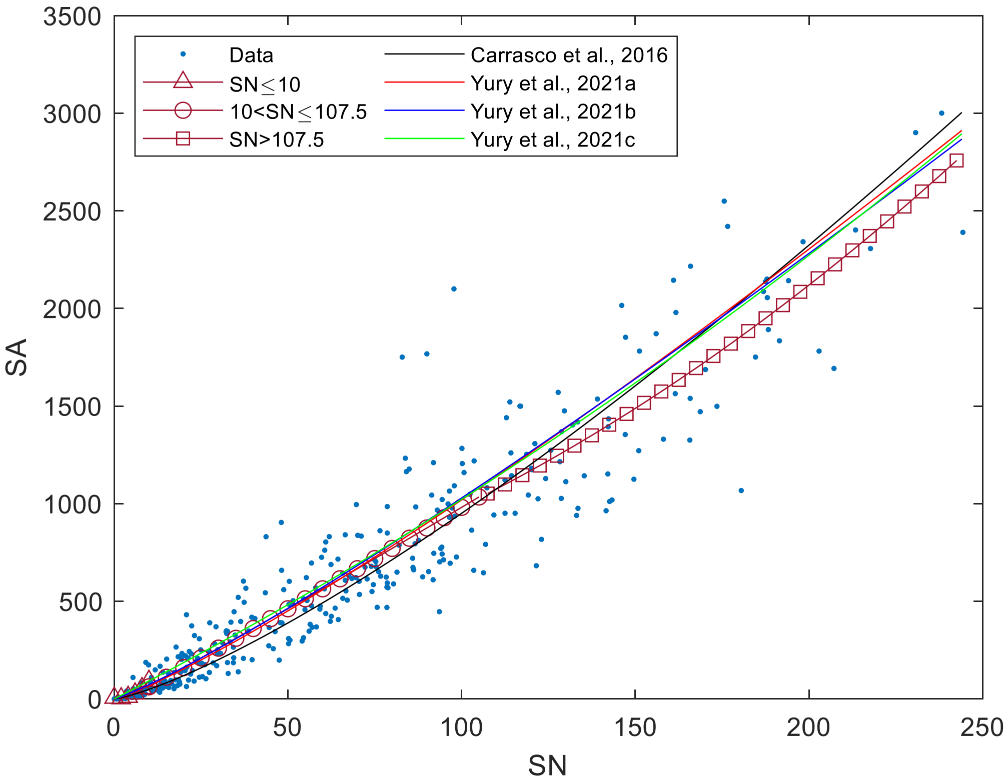

Fig. 10 Compare with other studies for the global data.

5. CONCLUSION AND DISCUSSION

The discussion about the characterization and the relationship between sunspot number and sunspot area for the two hemispheres would provide valuable insights into the behavior and the evolution of sunspots throughout the solar cycle.

Whichever hemisphere, the difference of sunspot number and sunspot area apparently shows the linear relation, no matter how the sunspot area varies with the sunspot number.

We could note there are obvious distinctions between the two hemispheres, through the distribution of sunspot number and area. We divided into 3 parts based on the number of sunspots to regress for exploring the relation between number and area. This way, we believe it could better reflect the correlations between sunspot area and number, especially in the low part and the high part. We could obtain a better regression result for these parts, data more or less static and data more discrete. This segmentation regression method will be conductive to convert the data from one to another, such as from sunspot number to sunspot area, a well-designed model be needed.

It is fair to say that the smooth transition at the junction between two parts has not discussed here. This question, and others, will be discussed in detail in the following articles of this series.

Sunspots are generally restricted to latitudinal bands some 30 degrees wide (Chang, 2018). The movement on the disk could be divided two important solar large-scale flow components: one is flowing in zonal direction with differential rotation, two is flowing to equator with meridional circulation, and then disappeared around equator (Charbonneau, 2020). With the solar differential rotation, the magnetic field line frozen within the fluid appears distortion along latitude, and shear rates vary in different dimensions. The gradients of change in velocity are the highest in 30^{o}, as well the strongest shear. Therefore, sunspots appear in the latitudinal bands some ≅30^{o} wide. At the same time, fluid flows along the longitude with meridional circulation with two components, from the high latitudes to the poles, and from the low latitude to the equator (Babcock. 1961). Therefore, if provide additional classifications of sunspot location for long enough to observe the ratio between the sunspot area and sunspot number, and see if we could spot patterns decreased in sequence towards to equator and the poles, 30^{o} as a dividing line. And we could go further about the asymmetry of the magnetic fields for the hemispheres.

ACKNOWLEDGMENTS:

This research has been supported by the National Natural Science Foundation of China (Grant No. 11203004). The data was provided by the Royal Greenwich Observatory and WDC-SILSO, Royal Observatory of Belgium, Brussels.

REFERENCES

Babcock, H.W.: 1961, The topology of the Sun's magnetic field and the 22-year cycle. Astrophys. J., 133, 572–587. DOI: 10.1086/147060

Carrasco, V.M.S., Vaquero, J.M., Gallego, M.C. and Sánchez-Bajo, F.: 2016, A normalized sunspot-area series starting in 1832: An update. Sol. Phys., 291, 2931-2940. DOI: 10.1007/s11207-016-0943-9

Casas, R., Vaquero, J.M. and Vazquez, M.: 2006, Solar rotation in the 17th century. Sol. Phys., 234, 379–392. DOI: 10.1007/s11207-006-0036-2

Chang, H.Y.: 2018, Latitudinal distribution of sunspot and North-South asymmetry revisited. J. Astron. Space Sci., 35, 55–56. DOI: 10.5140/JASS.2018.35.2.55

Charbonneau, P.: 2020, Dynamo models of the solar cycle. Living Rev. Sol. Phys., 17, 4. DOI: 10.1007/s41116-020-00025-6

Clette, F., Svalgaard, L., Vaquero, J.M. and Cliver, E.W.: 2014, Revisiting the sunspot number. Space Sci. Rev., 186, 1-4, 35–103. DOI: 10.1007/s11214-014-0074-2

Ermolli, I., Shibasaki, K., Tlatov, A. and van Driel-Gesztelyi, L.: 2014, Solar cycle indices from the Photosphere to the Corona: Measurements and underlying physics. Space Sci. Rev., 186, 105–135. DOI: 10.1007/s11214-014-0089-8

Hathaway, D.H.: 2010, The solar cycle. Living Rev. Sol. Phys., 7, 65 pp. DOI: 10.12942/lrsp-2010-1

Kiepenheuer, K.O.: 1953, Solar activity. In: The Sun, G.P. Kuiper (ed.). University Chicago Press, Chicago, 322–465.

Krivova, N.A., Balmaceda, L. and Solanki, S.K.: 2007, Reconstruction of solar total irradiance since 1700 from the surface magnetic flux. Astron. Astrophys, 467, 335–346. DOI: 10.1051/0004-6361:20066725

Nagovitsyn, Y.A. and Osipova, A.A.: 2023, Extreme values of sunspot activity on a long time scale. Astron. Lett., 49, 7, 421–429. DOI: 10.1134/S1063773723070034

Schröder, Wilfried: 1997, Some aspects of the earlier history of solar-terrestrial physics. Planet. Space Sci., 45, 3, 395–400. DOI: 10.1016/S0032-0633(96)00119-5

Solheim, J.-E., Stordahl, K. and Humlum, O.: 2012, The long sunspot cycle 23 predicts a significant temperature decrease in cycle 24. J. Atmos. Sol. Terr. Phys., 80, 267–284. DOI: 10.1016/j.jastp.2012.02.008

Waldmeier, M.: 1955, Results and problems of the solar research. 2nd ed., Leipzig, Geest und Portig, (in Germany).

Wolf, R.: 1861, Abstract of his latest results. Mon. Not. Roy. Astron., Soc., 21, 77. DOI: 10.1093/mnras/21.3.77

Yury, A., Nagovitsyn, A.A. and Osipova, A.: 2021, Average annual total sunspot area in the last 410 years: The most probable values and limits of their uncertainties. Mon. Not. Roy. Astron. Soc., 505, 1, 1206–1212. DOI: 10.1093/mnras/stab1328

Zhao, J. and Han, Y.B.: 2012, Sun's total irradiance reconstruction based on multiple solar indices. Sci. China-Phys. Mech. Astron., 55, 179–186. DOI: 10.1007/s11433-011-4496-5

Zharkova, V.V. and Shepherd, S.J.: 2022, Eigen vectors of solar magnetic field in cycles 21-24 and their links to solar activity indices. Mon. Not. Roy. Astron. Soc., 512, 5085–5099. DOI: 10.1093/mnras/stac781